Response times and energy partitioning in electron-beam-excited plasmas

Mark J. Kushner
University of Illinois, Department of Electrical and Computer Engineering, Gaseous Electronics Laboratory, 607 East Healey, Champaign, Illinois 61820

(Received 1 November 1988; accepted for publication 24 May 1989)

Excimer lasers are typically excited by electron beams (e beams) with initial energies of 100's of keV to a few MeV. The e-beam response time is the interval required for beam electrons and their energetic secondary electrons to slow below the first inelastic thresholds of the buffer gas, below which the electrons thermalize by elastic momentum transfer collisions. In this paper, e-beam response times for rare gases and for gas mixtures typically used for excimer lasers are discussed using results from a Monte Carlo simulation. Issues pertaining to energy partitioning (W values in mixtures and effective electron temperatures) are also discussed. We find that e-beam response times may be $>$ 10's of ns in gas mixtures of a few atm. As these times are commensurate with the rise time of e-beam pulses or the width of shorter pulses, beam slowing effects must be considered when modeling these phases of e-beam pumping.

I. INTRODUCTION

Electron beams (e beams) used to excite excimer lasers typically have initial energies of 100's of keV to a few MeV, and will slow in distances of 10's of cm at gas pressures of a few atm.[1–4] The deposition of energy in this manner can be viewed as the slowing of beam electrons by successive ionization and excitation collisions with the gas during which increments of energy are lost which are small compared to the beam electrons' initial energy. At energies greater than a few hundred eV, the beam electrons slow dominantly by ionization and transfer of energy to secondary electrons which are emitted having energies of 10's–100's of eV. Electron energy loss cross sections have their maximum values in the energy range in which secondary electrons are emitted. The cross sections typically scale as $\ln(\epsilon)/\epsilon$ at higher energies (ϵ is the electron energy). The fractional loss of energy by beam electrons therefore occurs slowly compared to secondary electrons. As a consequence, secondary electrons slow virtually instantaneously ($\ll$ 1 ns) at pressures exceeding a few atmospheres, whereas beam electrons with initial energies of $>$ 100's of keV may require 10's of ns to slow at the same pressures. For short or sharply rising e-beam pulses, these times may be significant fractions of the beam width or rise time.[5]

The power loss by both beam and secondary electrons depends critically on their position, in energy, with respect to the first inelastic threshold, ϵ_1, for collisions with the gas. At energies greater than ϵ_1, electrons dominantly lose energy in increments which are $\geqslant\epsilon_1$ (ionization or excitation to higher lying states). Below ϵ_1, electrons lose energy only by "elastic" collisions in increments which have an average value of $(2m_e/M)\epsilon$, where m_e is the electron mass and M is the atomic mass. The incremental energy loss is therefore small compared to ϵ_1. This latter process is commmonly called thermalization. The rate of energy loss therefore decreases sharply as electrons fall below ϵ_1. In atomic gases, the transition to thermalization may be quite abrupt. In molecular gases where inelastic electron loss by vibrational and rotational excitation may extend to below 1 eV, the onset of thermalization is less pronounced. The time required for the slowing of all beam and secondary electrons measured from the injection of the e beam to the onset of thermalization is defined here as the e-beam response time.

In this paper, we discuss e-beam response times for power deposition by electron beams in rare gases and in gas mixtures of interest to the excitation of excimer lasers. The response times were computed with a three-dimensional, time-dependent Monte Carlo simulation. We also discuss the effect of gas mixtures on W values (the energy expended to produce an ionization or excitation). We find that response times significantly increase with increasing beam energy, and decrease with decreasing W_i value (energy/ion pair). We also find that as a result of the differences in the rate of energy loss above and below ϵ_1, the residence time of electrons above ϵ_1 is shorter than below ϵ_1. Due to the predominance of attachment collisions below ϵ_1 in gas mixtures commonly used for excimer lasers, there is then a disparity between the times at which ionizations and attachments occur.

In Sec. II the slowing down model is described and the cross sections used in the calculations are listed. W values in gas mixtures are discussed in Sec. III, followed by a discussion of average electron energies in Sec. IV and e-beam response times in Sec. V. Concluding remarks are in Sec. VI.

II. DESCRIPTION OF THE SLOWING DOWN MODEL

The computer model used to calculate the e-beam response times is a three-dimensional time-dependent Monte Carlo particle simulation. It is conceptually similar to other Monte Carlo models[6–8] and therefore will be only briefly described here.

Prior to beginning the slowing down calculation, a gas mixture is selected and the energy range of interest is divided into bins centered at ϵ_i. The total electron collision frequency in each energy interval, ν_i, is determined and probability arrays are initialized for each energy interval. The probability arrays are denoted P_{ij}, for energy i and collision process j. They have the properties that

$$P_{ij} = \frac{\nu'_{ij}}{\nu_i}, \quad \nu'_{ij} = \sum_{l=1,j} \nu_{il}, \tag{1}$$

where ν_{ij} is the collision frequency for energy interval i and

 0021-8979/89/182297-10$02.40

process j, ν'_{ij} is the cumulative collision frequency for processes $l \leqslant j$, and P_{ij} is normalized so that for m processes, $P_{im} = 1$. The simulation then begins by giving a beam electron energy ϵ_0 and a direction perpendicular to the electron gun foil.

In the absence of an applied electric field, an electron's energy changes only by collisions. The choices of which collision occurs and the time between collisions are made by selecting a series of pseudo random numbers $r_i = (0,1)$. The time interval to the next collision for an electron with energy ϵ_1 is given by $\Delta t = -\ln(r_1)/\nu_i$. The type of collision that occurs at that time is the process that satisfies $P_{i,j-1} < r_2 \leqslant P_{i,j}$ where j is the collision which occurs and r_2 is a second random number. The time of flight and position of the electron are revised according to Δt, and the energy of the electron is revised to $\epsilon \rightarrow \epsilon - \Delta\epsilon_{ij}$, where $\Delta\epsilon_{ij}$ is the energy loss associated with process j at energy i. The velocity of the electron is updated based on a collision whose scattering angles are azimuthally symmetric ($\phi = r_3 2\pi$) and whose polar angle is confined to a specified interval ($\theta = r_4 \Delta\theta$). The location, time, energy deposition, and type of the collision are recorded, and the next flight computed.

In the event that the collision is an ionization the energy loss includes the kinetic energy of the secondary electron. The energies of the secondary electrons are randomly selected from the distributions of Opal, Peterson, and Beaty.[9] We assume the secondary electrons are emitted isotropically. The secondary electron distribution was approximated as

$$f(\epsilon_s) \sim \frac{1}{1 + (\epsilon_s/\bar{\epsilon})^2}, \tag{2}$$

where ϵ_s is the secondary electron energy and $\bar{\epsilon}$ depends on the gas. For a maximum secondary electron energy of $\epsilon_s = (\epsilon_p - \epsilon_{\text{ion}})/2$ (ϵ_p is the primary energy), this function may be easily inverted to yield the randomly selected secondary energy

$$\epsilon_s = \bar{\epsilon} \tan[r_5 \, a \tan(\epsilon_p - \epsilon_{\text{ion}}/2\bar{\epsilon})]. \tag{3}$$

The location, time of emission, and energy of the secondary electron are recorded for later use.

The beam electron is followed until it leaves the boundaries of the system, attaches, recombines, or falls below some minimum energy of interest. At that time, a secondary electron is selected from the record of their emission times, locations, and energy, and its flight is computed until it too is lost from the system as described above. Additions are made to the stack of secondary electrons as the second generation electrons themselves have ionization collisions. The process continues until the "stack" of secondary electrons is exhausted, at which time a new beam electron is started. For initial beam energies in excess of 200–300 keV, typically only 2–10 beam electrons are necessary to obtain acceptable statistics.

The electron distribution function may be obtained from the slowing down calculation by summing the collision events occuring at a particular energy and weighting each contribution by the time of flight for that collision. In the absence of processes which depend upon the electron density, the distribution function so calculated is exact. In the presence of such processes, such as electron-electron collisions, the distribution function cannot be so obtained. Under these collisions, the Monte Carlo slowing down calculation was used to calculate the energy dependent influx of electrons arriving below a preselected energy, typically 50 eV. This influx was then used as the source term in solving Boltzmann's equation for the electron distribution function while including electron-electron and superelastic collisions. Boltzmann's equation was solved by essentially the same method as described by Bretagne, Godart, and Puech.[10] The sources of our cross sections are listed in Table I.[11-19] High-energy extrapolation of ionization and allowed excitations was performed using $\ln(\epsilon)/\epsilon$ scaling.

TABLE I. References for sources of cross sections.

Gas	Momentum transfer	Excitation	Ionization
He	Ref. 11	Ref. 7	Ref. 19
Ne	Ref. 11	Refs. 13, 14	Ref. 19
Ar	Ref. 11	Ref. 15	Ref. 19
Kr	Ref. 11	Ref. 16	Ref. 19
Xe	Ref. 11	Refs. 17, 18	Ref. 19
F_2	Ref. 12	Ref. 12	Ref. 12

III. W VALUES IN GAS MIXTURES

As a method of validating the e-beam energy deposition portion of the model, we calculated W values for pure rare gases and for rare gas mixtures. Recall that the W value is the energy invested in the plasma to obtain a specific electron impact event (either an ionization or an excitation). W values are the common method of partitioning energy deposition by highly energetic particles.[20] The W values we discuss here are for only the excitation and ionization caused by the slowing of beam electrons and their progeny. We do not discuss the subsequent partitioning of that energy by heavy particle reactions because those subsequent reactions depend upon case specific parameters. For example, the formation of an excited state of He by a beam electron in a He/Xe mixture could ultimately lead to a xenon ion by a Penning reaction. The He* atom, though, could also decay by superelastic collisions with thermal electrons and or dimerize to He_2^* leading to radiative decay. The relative frequency of these processes depend upon the thermal electron density (i.e., power deposition) and absolute pressure. The rates of ionization and excitation one obtains from W values in any mixture except pure gases should be considered as source terms for beam electrons in the rate equations for the species in question. The rate equations would also include other case specific reactions (e.g., Penning reactions, dimerization, thermal electron collision quenching) which do not directly depend upon the beam parameters.

In our calculations, we confirmed the observation of other investigators that W values are relatively insensitive to the beam energy for values exceeding a few keV.[1] This condition results from the fact that the convolution of the secondary electron spectrum and excitation cross sections are relatively insensitive to the primary energy for ϵ_0 greater than a few keV. Also the distribution of excitations and ionizations for a primary electron with, for example, $\epsilon_0 = 200$ keV

TABLE II. W values and total excitation for rare gases.[a]

		W_{ion} (eV)					W_{exc} (eV)					Total excitations and ionizations for 100 eV				
	Ref.	He	Ne	Ar	Kr	Xe	He	Ne	Ar	Kr	Xe	He	Ne	Ar	Kr	Xe
Christophorou	21	46.0	36.6	26.4	24.0	21.7										
Janciatis	22	42.6	36.8	29.4	23.0		83.5	78.3	55.5	41.8		3.54	3.99	5.20	6.74	
Kannari	1		38.0	25.0	21.0	22.0		67.9	55.6	63.6	57.9		4.11	5.80	6.33	6.27
Lorentz	20			26.2	24.3	21.9			93.6	69.4	48.7			4.89	5.56	6.62
Blauer[b]	23	46.0	36.6	26.4	24.0	21.7	85.2	110.9	82.5	61.5	42.5	3.35	3.63	5.00	5.79	6.96
This work		46.8	36.5	27.3	23.6	20.9	72.0	81.8	53.8	44.5	34.8	3.53	3.96	5.52	6.48	7.66

[a] W_{ion} ≡ energy per ionization. W_{exc} ≡ energy per excitation for all states.
[b] Values used for W_{ion} were those of Ref. 21.

differs from that with $\epsilon_0 = 100$ keV only during its slowing between the two values; hence, the differences in W values should not be expected to be large.

W values for ionization, total excitation and the total number of excitations and per 100 eV deposited for rare gases are listed in Table II using the results for this study and those from other sources.[21–23] In general, we find good agreement between the different sources for ionization. There are no systematic differences in W values for ionization between the various works. We do, though, find systematic trends in the results of theoretical works in which both ionization and excitation processes are considered (Refs. 1, 22, and this work). If a W value for ionization is higher than the average (that is, less ionization per unit energy) then the W value for excitation is low (that is, more excitation per unit energy). The effects are compensating so that the total sum of excitations and ionizations per unit energy is roughly the same. The energy that is not expended in ionization results in excitation. The system would be absolutely conservative if not for secondary electrons which are emitted below the first inelastic threshold, ϵ_1. The differences between W values for excitation and ionization between workers is therefore a result of the relative differences between ionization and excitation cross sections used by those workers (for theoretical values). The differences seen between the *total* sum of excitation and ionization events are a result of differences in the fraction of the secondary electrons which are emitted below the first inelastic threshold energy, ϵ_1, as the energy of those electrons is wasted with respect to further excitation. As an added observation, we find that treatments which simultaneously consider excitation, ionization, and secondary electron distributions tend to yield lower W values for excitation than those which base excitation yields on an average secondary electron energy.[20,23]

The use of W values in gas mixtures must be done on a case by case basis because there is no straightforward correlation between the W values in the mixture and those for the pure gases.[1,22] In the following we define the W values for the pure gas i as W_i^0. The W value for that gas in a mixture, W_i, should scale roughly as W_i^0/f_i, where f_i is the mole fraction of gas i. This relationship is merely a statement that the probability of intercepting energy scales with the relative amount of gas of that type in the mixture. Due to competition between electron impact processes near threshold and the disparity in the magnitude of electron impact cross sections at higher energies, we find that generally $W_i^0 \neq f_i W_i$. This discrepancy increases dramatically as the ionization potentials of the constituents diverge.

Eggarter,[24] and Inokuti and Eggarter[25] investigated the initial yield of ions in Ar/H_2 mixtures. They suggest that W values in binary mixtures can be obtained from

$$1/W = (Z/W_1^0) + [(1-Z)/W_2^0], \tag{4}$$

$$Z = \frac{f_1}{f_1 + (W_2^0/W_1^0)(\sigma_2/\sigma_1) f_2}, \tag{5}$$

where σ_i is the ionization cross section for species i evaluated at an energy in the asymptotic regime ($\epsilon \gtrsim 1000$ eV). Although they obtained good agreement for this scaling with detailed calculations for Ar/H_2 mixtures, we found that the scaling was less applicable to species whose ionization potentials are significantly different. This scaling also does not directly translate to gas mixtures with more than two components. Therefore further investigation is warranted.

W values for ionization and excitation in $Ar/Kr/F_2$ gas mixtures, as commonly used for e-beam pumped KrF lasers, are plotted in Fig. 1. As one might expect, the W values for Ar increase with decreasing Ar mole fraction, as more energy is intercepted by Kr [see Fig. 1(a)]. The mole fraction weighted W values, $f_i W_i$, though, are not a constant as would be the case if power deposition was partitioned by fractional density [see Fig. 1(b)]. We find that the mole fraction weighted W values for ionization of both Ar and Kr increase with increasing Kr mole fraction. This scaling is counterintuitive, as one would expect that the W value for Kr would decrease as its mole fraction increases. This effect is more dramatically seen with mole fraction weighted W values for ionization in $He/Xe/F_2$ gas mixtures [Fig. 2(a)]. In this mixture the differences in ionization potentials of the constituents are greater than for the Ar/Kr mixtures. In fact, the mole fraction weighted W values for Xe are less than the ionization potential of xenon for mole fractions less than 0.6. Under these conditions, the scaling suggested by Inokuti and Eggarter is less accurate, as shown in Fig. 2(b). Here the difference in ionization resulting from secondary electrons near threshold is an appreciable fraction of the total.

These trends in W values can be understood by viewing the mole fraction weighted W values as the incremental ener-

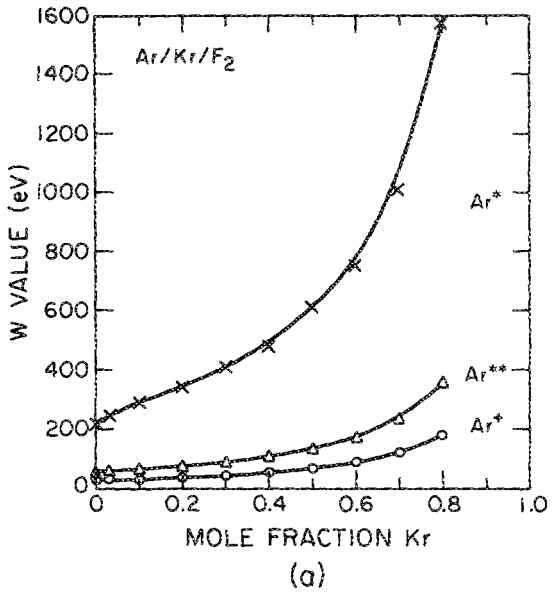

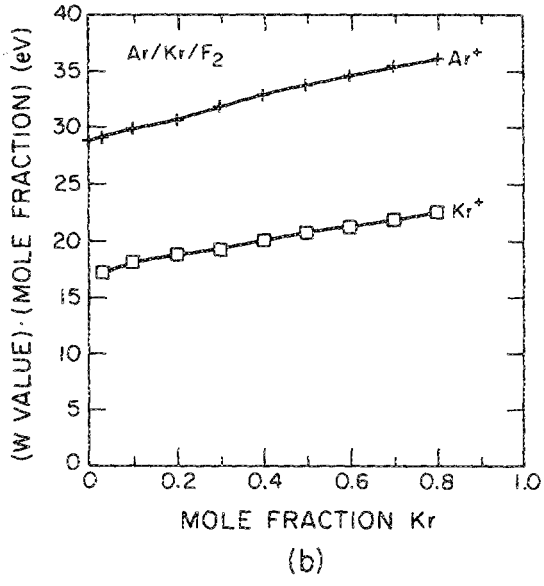

FIG. 1. W values (eV/event) for an $Ar/Kr/F_2$ gas mixture as a function of Kr mole fraction for an e-beam energy of 500 keV. The F_2 mole fraction is constant at 0.25%. (a) W values for excitation and ionization of argon. (b) Mole fraction weighted W values (mole fraction $\times$ W value) for ionization of Kr and Ar. Note that the mole fraction weighted W value increases for both Kr and Ar in spite of the increase in Kr mole fraction. W values therefore do not simply scale with mole fraction.

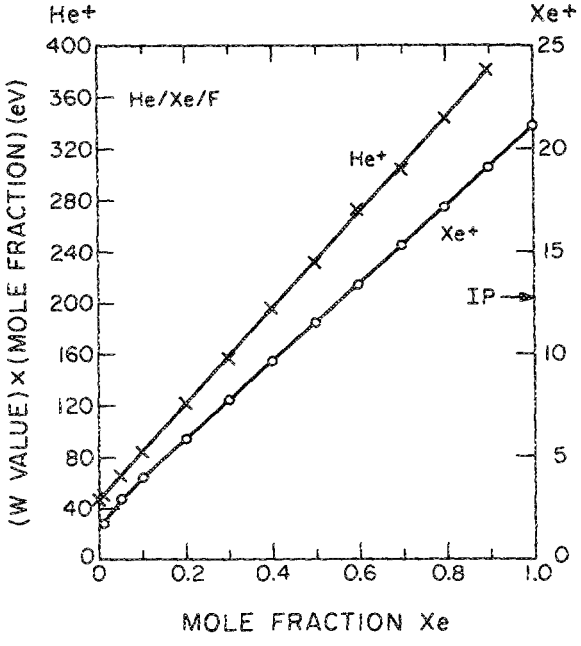

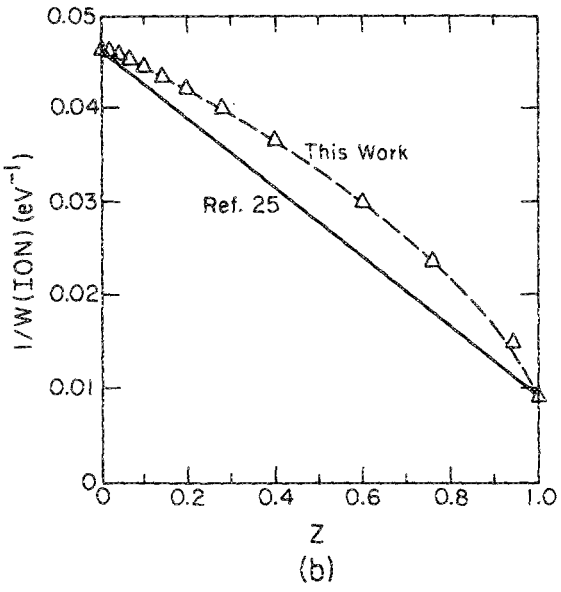

FIG. 2. (a) Mole fraction weighted W values (mole fraction $\times$ W value) for ionization of He (left scale) and Xe (right scale) in a $He/Xe/F_2$ mixture as a function of Xe mole fraction. The beam energy is 500 keV and the F_2 mole fraction is constant at 0.25%. The mole fraction weighted W value for ionization of Xe can be significantly less than its ionization potential (12.1 eV, shown by an arrow on the right scale) due to the lack of competition with He below its electronic threshold energy (19.8 eV). (b) Comparison of $1/W$ obtained by this method and that of Inokuti and Eggarter (Ref. 25) for a He/Xe mixture. Z is the parameter defined by Eq. (5) with $Z = 0$ corresponding to pure xenon. The cross sections in Eq. (5) were evaluated at 1000 eV.

gy that must be invested in the plasma to obtain the desired product. Consider the example of a gas mixture with two components where the ionization potential of one gas is less than the first inelastic threshold of the second. This is the case for mixtures of Xe and He. If the mole fraction of Xe is sufficiently small, then competition between Xe and He at energies above the inelastic threshold of He (19.8 eV) can be ignored. Electrons which fall below the first inelastic threshold of He are no longer useful for exciting He. These electrons can, though, still excite and ionize Xe (8.3 and 12.1 eV, respectively). Therefore, the incremental amount of energy necessary to obtain an additional ionization or excitation from xenon is negligible, and the mole fraction weighted W value will be proportionally small. As the mole fraction of xenon increases the competition between Xe and He increases at higher energies. The mole fraction weighted W value then increases for both species. The disparity between $f_i W_i$ and W_i^0 is a measure of the competition, or lack thereof, between the constituents of the gas mixture. This disparity is exemplary of the need to calculate W values on a case by case basis.

IV. AVERAGE ELECTRON ENERGY

In *e*-beam excited excimer lasers, ionization and excitation processes from the ground state are dominated by the slowing of beam electrons. The bulk electrons are those electrons having energies less than the first inelastic thresholds, from the ground state, of the noble gases. In contrast, bulk electrons are most important in electron-ion recombination, electron attachment, electron collision quenching, and excitation or ionization collisions with excited states. There have been many studies of the time development of the electron distribution function in *e*-beam excited plasmas and it is well known that at low electron densities ($n_e/N < 10^{-5}$) the distribution function may be non-Maxwellian, and rate constants obtained by assuming so may not be accurate.[1,10,26,27] At higher electron densities, electron-electron collisions thermalize the distribution and a Maxwellian distribution is not a bad approximation. In either case, the characteristic electron temperature ($T_e = \frac{2}{3}\langle\epsilon\rangle$) is the same since electron-electron collisions do not significantly change this value for these conditions.[27]

As a practical matter many models for electron beam pumped plasmas will continue to use electron collision rate coefficients which are functions of T_e since calculating the electron distribution function is impractical or not necessary for their conditions. Although the precise value of T_e used in the model is important, there are no accepted values of T_e used in published models of *e*-beam excited plasmas. The values so used range from 1 to 2 eV.

In this respect, we present values of T_e calculated with the Monte Carlo simulation. These values are presented in Table III for $M/F_2 = 99.75/0.25$ rare gas mixtures as being representative of those used in excimer lasers. The electron temperatures are relatively insensitive to *e*-beam energies of 60 keV–1 MeV, increasing by only a few percent over this range. With the exception of Ne, T_e decreases from He to Xe with all values being in the range of 1.25–1.5 eV. The electron temperature for Ne is higher due to its lower momentum transfer cross section at energies < 10 eV compared to He.[11] The electron temperature is, though, sensitive to the mole fraction of F_2 (see Fig. 3) in the gas mixture. The average electron energy is largely determined by the energy at which electron loss occurs. Attachment by F_2 at low energy increases the average electron energy due to loss of those low-energy electrons. This electron loss is shown by the decrease in the electron distribution function at $\epsilon < 2$ eV where the attachment cross section peaks [see Fig. 3(b)]. In the range of typical F_2 mole fractions used in excimer gas mixtures ($5\times10^{-3} \leqslant f_{F_2} \leqslant 5\times10^{-2}$) the electron temperature ranges from 1.4 to 1.6 eV.

TABLE III. Effective electron temperature (eV) for rare-gas mixtures $M/F_2 = 99.75/0.25$.

M	T_e[a]
He	1.49
Ne	1.63
Ar	1.43
Kr	1.41
Xe	1.34

[a] $T_e = \frac{2}{3}\langle\epsilon\rangle$ where $\langle\epsilon\rangle$ is the average electron energy.

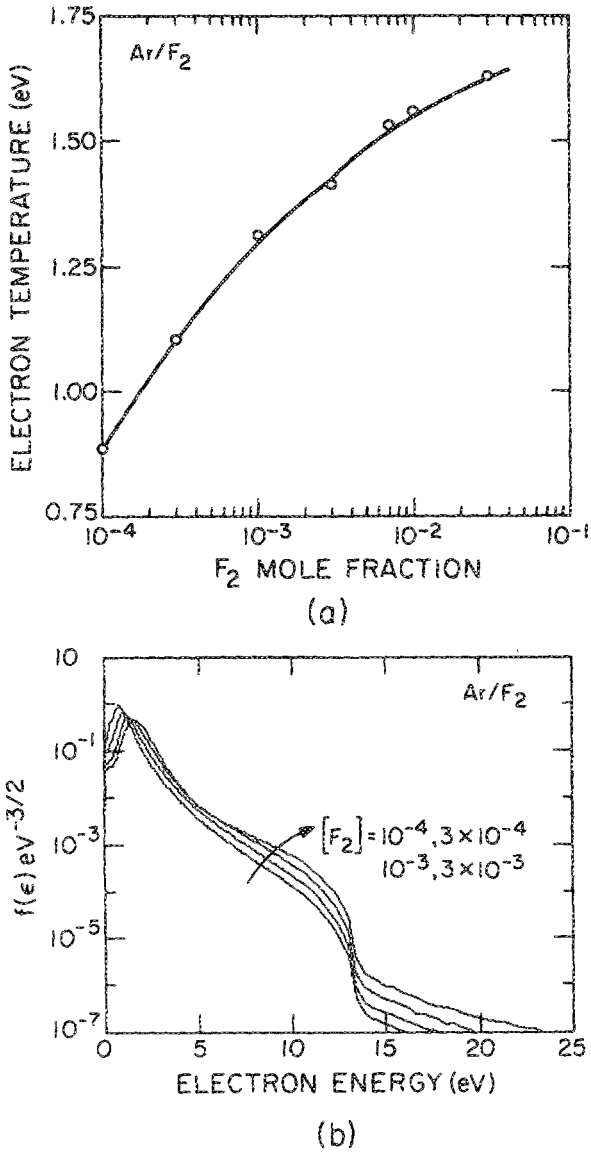

FIG. 3. Bulk electron parameters for slowing of a 500-keV electron beam in an Ar/F_2 mixture as a function of F_2 mole fraction; (a) effective electron temperatures ($T_e = \frac{2}{3}\langle\epsilon\rangle$), and (b) electron distribution functions. The electron temperature increases with increasing F_2 mole fraction due to the attachment of low energy electrons, shown by the decrease in the distribution function at $\epsilon \leqslant 2$ eV. The tail of the electron distribution at $\epsilon > 15$ eV is due to the influx of slowing beam and energetic secondary electrons.

As is true for W values, electron temperatures may not simply scale in mixtures from their pure gas values. It is well known from low-energy electron swarm studies that electron transport coefficients in a mixture may in fact be quite different than either of the constituents at the same E/N.[28] We also observe this behavior for the bulk electron temperature of some *e*-beam pumped plasmas. This behavior is shown in Fig. 4 where T_e is plotted for a $He/Xe/F_2$ gas mixture as a function of Xe mole fraction. T_e is a minimum at a xenon mole fraction of $\simeq 20\%$, where the secondary electron spectrum matches the thresholds of xenon excitation cross sections, and results in a larger influx of electrons

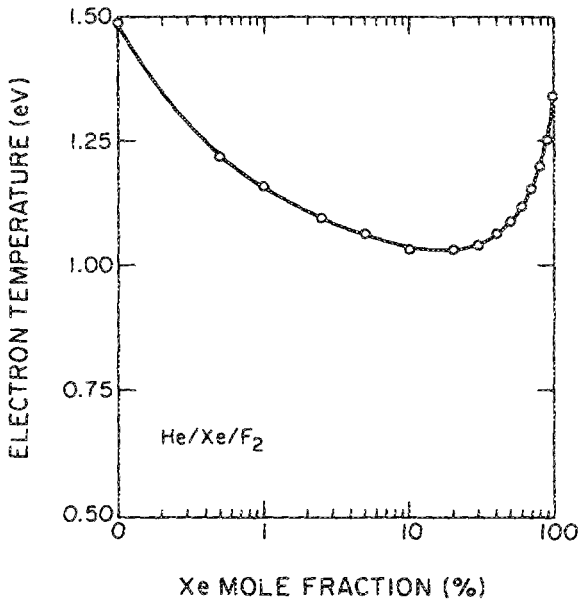

FIG. 4. Effective electron temperatures ($T_e = \frac{2}{3}\langle\epsilon\rangle$) as a function of Xe mole fraction in a He/Xe/F_2 mixture for an e-beam energy of 500 keV. The F_2 mole fraction is constant at 0.25%.

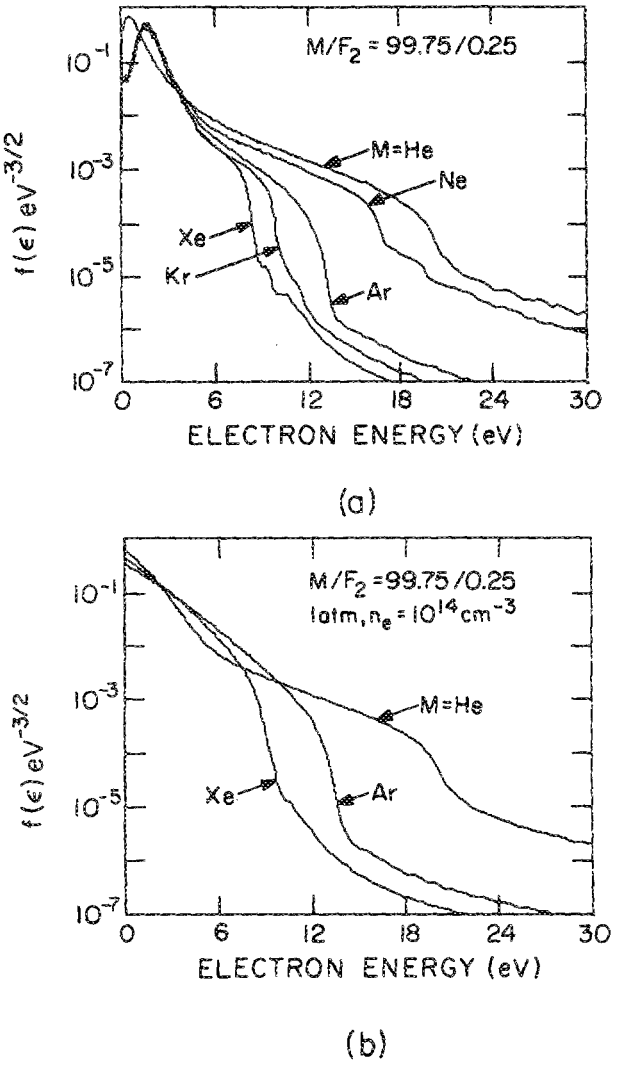

FIG. 5. Electron distribution functions for the bulk electrons in M/F_2 = 99.75/0.25 mixtures (M = He, Ne, Ar, Kr, Xe); (a) negligible electron density, and (b) $n_e = 1\times10^{14}\,\mathrm{cm}^{-3}$ at 1 atm (fractional electron density $= 5\times10^{-6}$). Only moderate electron densities are required to thermalize the electron distribution at low energies, $\epsilon < \epsilon_1$ (the first electronic excitation threshold of the rare gas). The high-energy tails of the distribution functions result from the influx of slowing beam electrons and energetic secondaries.

at lower energies. As the momentum transfer cross section of xenon is large compared to He, this effect persists to low Xe mole fractions.

Although the electron temperatures are all similar for the rare gases, the electron distribution functions for the bulk electrons ($\epsilon \lesssim 20$–30 eV) are dramatically different, particularly for $\epsilon > 5$–10 eV (see Fig. 5). Exemplary electron distribution functions are shown in Fig. 5(a). The cutoffs in the distribution functions are at successively lower energies in going from He to Xe, a consequence of successively smaller values of ϵ_1. The high-energy tails to the distributions are due to the influx of slowing beam electrons and their high-energy secondaries. The differences in the electron distribution functions are less pronounced, though, at higher-power deposition where the electron density exceeds $n_e/N > 10^{-5}$ and when electron-electron thermalization is important [see Fig. 5(b)]. The decrease in $f(\epsilon)$ at low energy due to attachment is mitigated, but the cutoff in the distributions persist. Electron impact rate coefficients for processes with thresholds greater than 5–10 eV are therefore not well represented by the Maxwellian approximation even at high electron densities. In practice, though, the error in calculating electron impact rate coefficients for high threshold processes for allowed transitions or ionization using a Maxwellian is not particularly damaging. These processes have peaks in their cross sections at 10's–100's of eV. They are therefore dominated by slowing beam electrons and secondaries, and not by the bulk electrons so the error in their rate coefficients makes a relatively small contribution.

V. *e*-BEAM RESPONSE TIME

The e-beam response times we discuss here are those values one would observe by averaging the electron distribution over a system large enough to slow the beam electrons without their striking the walls. The local response time, though, may be quite different. Take, for example, the case of a monoenergetic e beam passing through a small observation volume generating a spectrum of secondary electrons. The response time in the observation volume is very short since the electrons which slow in the volume consist only of the secondaries born with energies of less than a few hundred eV (see below). The response time averaged over the slowing down volume, including the beam electrons, can be significantly longer.

The electron energy spectrum for the slowing of a 500-keV e beam having a current pulse of 5 ns (FWHM) is shown in Fig. 6 as a function of time for a 1-atm gas mixture typically used for e-beam-excited KrF lasers (Ar/Kr/F_2 = 90/10/0.25). The figures show the fractional density of electrons at a particular energy and time for $\epsilon \lesssim 200$ eV [Fig. 6(a)] and $\epsilon \lesssim 30$ eV [Fig. 6(b)]. Note that the higher-

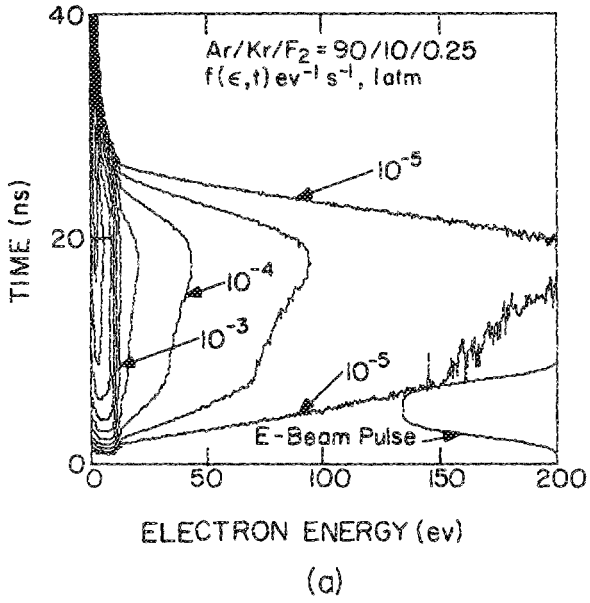

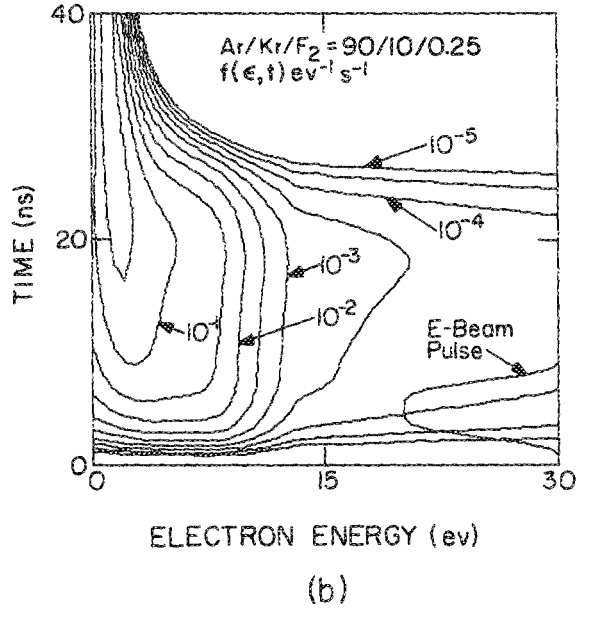

FIG. 6. The electron spectrum as a function of energy and time ($eV^{-1}\,s^{-1}$) for a 500-keV *e*-beam pulse (5-ns FWHM) slowing in a 1-atm Ar/Kr/F_2 = 90/10/0.25 mixture; (a) $0 \leqslant \epsilon \leqslant 200$ eV, and (b) $0 \leqslant \epsilon \leqslant 30$ eV. The time dependence of the *e*-beam pulse is at the bottom right in each figure. The *e*-beam response time for these conditions is $\simeq 20$ ns. Note the transition to thermalization at 20–30 ns.

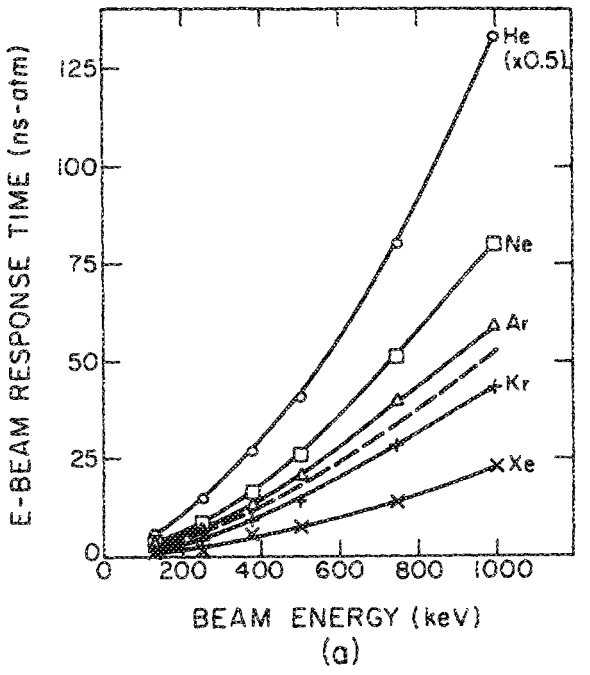

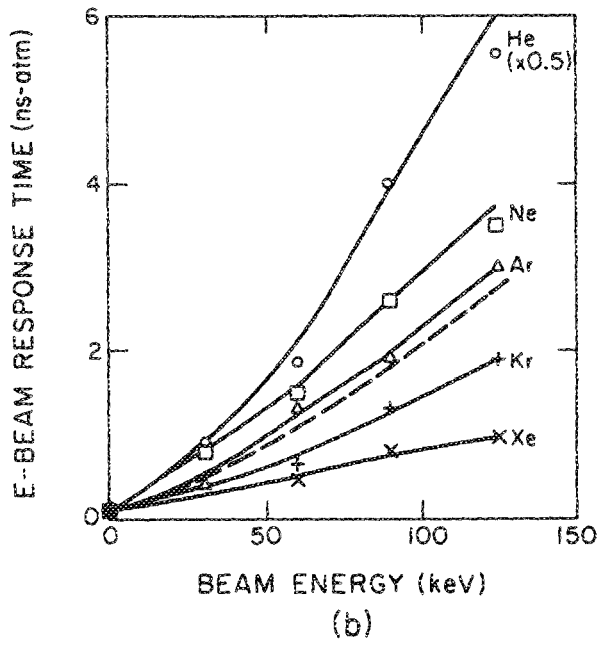

FIG. 7. *e*-beam response times (ns atm) as a function of electron beam energy for the rare gases: (a) 150 keV $\leqslant \epsilon_0 \leqslant 1$ MeV, and (b) $\epsilon_0 \leqslant 125$ keV. The response times for He have been divided by two for presentation purposes. The dashed line is the beam response time for Ar obtained while explicitly including the *L*-shell ionization.

energy spectrum consists dominantly of secondary electrons generated by the beam electrons. The direct contribution of the beam electrons is small since each beam electron ultimately is responsible for $> 10^4$ secondaries. The *e*-beam response time is the delay between beam injection and slowing down of the beam electrons and their progeny below the major inelastic thresholds. The response is approximately 20 ns for these conditions at 1 atm. An elapsed time of almost 30 ns at 1 atm is required for the medium to respond to the 5-ns FWHM *e*-beam pulse. The transition to thermalization, and reduction in power loss is clearly shown in Fig. 6(b) at $t \approx 30$ ns.

e-beam response times as a function of beam energy for the rare gases are shown in Fig. 7. These values were obtained by using a delta-function *e*-beam pulse at $t = 0$, and observing the analogous point as noted in Fig. 6. The response times are given in units of ns atm (i.e., longer response times at lower pressures). The response times increase nearly linearly with increasing beam voltage. These beam response times were obtained using the total ionization cross section of Ref. 19 which contains contributions from ionization of, for example, both the *M* and *L* shells of Ar. Since the threshold energy for ionization of inner shell elec-

trons is larger than that of the outer shells, the rate of energy loss should be higher, and response time shorter, when explicitly including the inner shell process. To evaluate this effect, the contribution of the L-shell ionization to the total ionization cross section of Ar was included (threshold energy 250 eV) in the analysis using the partial cross section and secondary electron spectrum of Peterson and Allen.[29] The L-shell ionization cross section has a maximum value of $\approx 6\times 10^{-19}$ cm^2 at 800 eV compared to a maximum value of 4×10^{-16} cm^2 at ≈ 100 eV for the total ionization cross section. The additional energy loss from L-shell ionization decreases the response time for argon by $\approx 12\%$ for a beam energy of 1 MeV, and 7% at 125 keV, as shown by the dashed line in Fig. 7.

The rate of energy loss, and hence beam response time, is also sensitive to the contributions of the partial cross sections for multiple ionizations to the total ionization cross section (e.g., $e + \mathrm{Ar} \rightarrow \mathrm{Ar}^{2+} + 3e$). The partial ionization cross sections for the rare gases are generally only known for energies <15–20 keV.[30] At 14 keV, the fractional contributions of higher ionization for the rare gases are 0.027, 0.026, 0.064, 0.14, and 0.19 respectively for He, Ne, Ar, Kr, and Xe.[30] These contributions are approximately constant for energies $\gtrsim 5$ keV. As the secondary electron spectra for multiple ionizations are generally not known, it is difficult to assess the effect of multiple ionizations on the beam response time. By energy and momentum conservation arguments, one would expect that the sum of the secondary electron energies in double ionizations to be less than twice that for a secondary electron in a single ionization. Therefore, the total rate of energy loss including the partial contributions of multiple ionizations is likely not to be significantly different from that obtained using the total ionization cross section and assuming single ionizations. In any case, the increase in the rate of energy loss is at most a 10% when assuming the same secondary energy for each electron.

e-beam response times may also be estimated by integrating the relativistic stopping power, $d\epsilon/dx$, from injection energy to a few keV. This was done using the Bethe stopping power theory[31] for comparison to this method. The values so obtained were smaller than those obtained with this method by the following ratios: approximately 0.95, 0.7, 0.68, 0.45, and 0.6, for He, Ne, Ar, Kr, and Xe. The differences cannot be attributed to improper partitioning of e-beam energy for either primary or secondary electrons as confirmed by the good agreement obtained for W values. In fact, increasing the energy loss to secondary electrons to decrease the response time gives poor agreement for W values, as does increasing the energy loss to radiation. The differences are most likely a result of two causes: differences in the high-energy asymptotic form of the cross sections, and inappropriate representation of multiple ionizations by the total ionization cross section. If the latter effect is dominant, then according to the arguments above the secondary electron spectrum for each secondary electron during a multiple ionization must be nearly the same.

Response times are shown in Fig. 8 for $\mathrm{He/Xe/F_2}$ and $\mathrm{Ar/Kr/F_2}$ mixtures. Since the slowing down characteristics of Ar and Kr are separately similar, the e-beam response

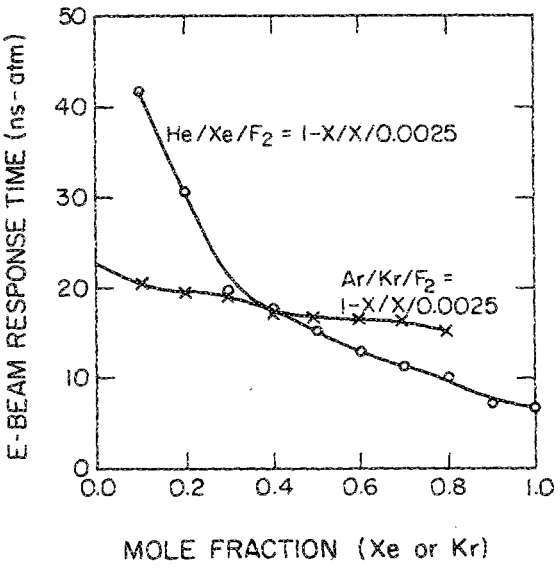

FIG. 8. e-beam response times (ns atm) for $\mathrm{Ar/Kr/F_2}$ and $\mathrm{He/Xe/F_2}$ mixtures as a function of Kr or Xe mole fraction. The electron beam energy is 500 keV and the F_2 mole fraction is constant at 0.25%. The response time for $\mathrm{Ar/Kr/F_2}$ mixtures is relatively constant as the gas mix is varied. The response time for the $\mathrm{He/Xe/F_2}$ mixture decreases significantly with increasing Xe mole fraction as a result of the larger stopping power of Xe.

times are not dramatic functions of Kr mole fraction. The response time does decrease with increasing Kr fraction since its stopping power is larger. For the $\mathrm{He/Xe/F_2}$ mixture, the large difference in stopping power between He and Xe causes a dramatic dependence of e-beam response time on Xe mole fraction, decreasing from >40 ns atm for $f_{\mathrm{Xe}} = 0.2$ to $\leqslant 10$ ns atm for $f_{\mathrm{Xe}} = 1.0$.

As beam and secondary electrons cascade in energy below the inelastic thresholds, the rate of energy loss decreases significantly. This condition implies that for short e-beam pulses, the times at which high threshold events occur are different than that for low threshold events. This effect is shown in Fig. 9(a) where the time distribution for ionization and attachments are shown relative to the e-beam pulse for the conditions of Fig. 1 (1 atm, $\mathrm{Ar/Kr/F_2} = 90/10/0.25$, $\epsilon_0 = 500$ keV, e-beam pulse 5-ns FWHM). The ionization cross sections are maximum at ≈ 100–200 eV, while the attachment cross sections are maximum at $\epsilon = 0$ and effectively negligible at ϵ greater than a few eV. The peak in the number of ionizations is displaced from the peak in the e-beam pulse by ≈ 12–15 ns, implying that approximately that amount of time is required for primary and secondary electrons to cascade from higher energies to the peak in the ionization cross sections. The prompt attachments result from secondary electrons which are emitted at energies coincident with the attachment cross sections. The increase in attachment events and their presence far after the cessation of ionizations are a result of the finite times required for electrons to traverse, in energy, the region between the inelastic thresholds and the attachment cross sections. Since the e-beam response time varies inversely with pressure, the disparity between beam injection and ionization (or ionization and attachment) is also a function of pressure. In Fig. 9(b)

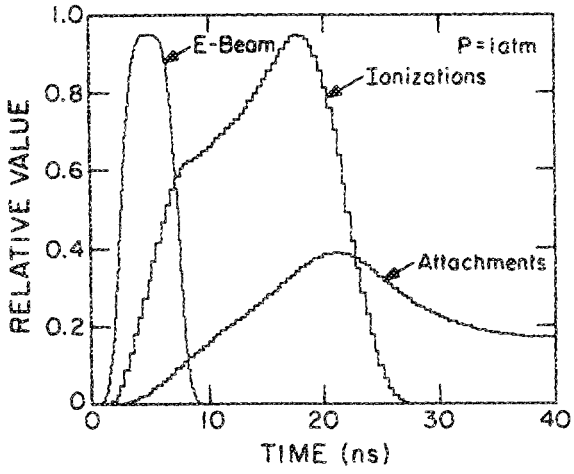

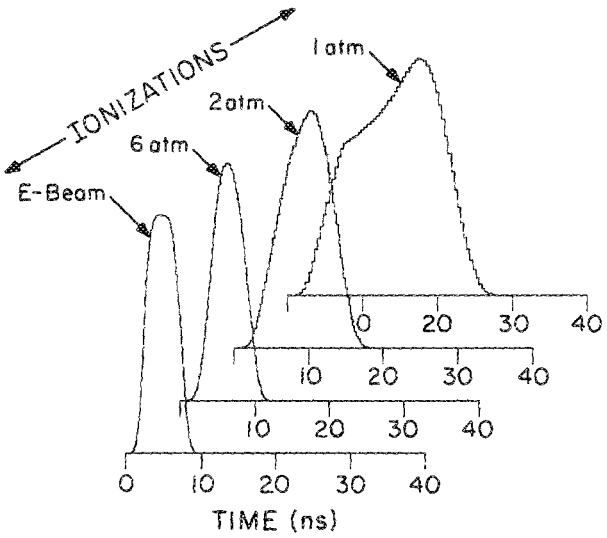

FIG. 9. The time dependence of electron collisions following a 500 keV electron beam pulse (5-ns FWHM) in an $Ar/Kr/F_2 = 90/10/0.25$ mixture. (top) Ionization and attachment events in a 1-atm mixture. Attachment cross sections are important only for $\epsilon < 2$ eV. Since thermalization is slow once electrons fall below the electronic thresholds of the buffer gas, there is a disparity in time between when ionizations and attachments occur. (bottom) Ionization events at pressures of 1, 2, and 6 atm. The *e*-beam response time at 6 atm is sufficiently small that ionizations track the *e*-beam current.

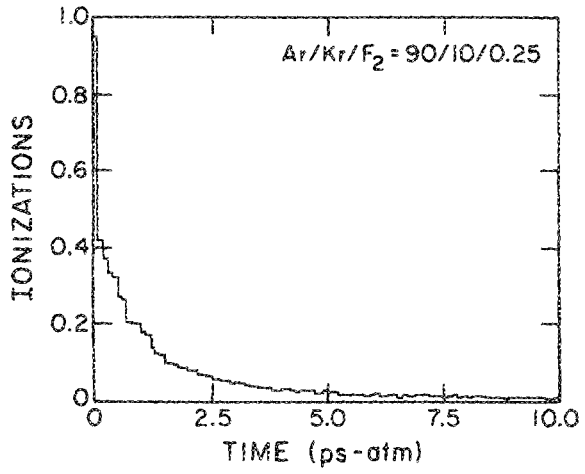

FIG. 10. The time dependence (ps atm) of ionizations resulting from the secondary electrons generated by a 500-keV electron-beam pulse passing through a small observation volume. The gas mixture is $Ar/Kr/F_2 = 90/10/0.25$. Due to the larger energy loss cross sections at the energies at which secondary electrons are emitted, they slow quickly compared to the beam electrons.

we show the ionization events for a 5-ns FWHM *e*-beam pulse as a function of gas pressure. For pressures exceeding 4–5 atm, the time dependence of ionizations is indistinguishable from the *e*-beam pulse. This is a consequence of the *e*-beam response time becoming small compared to the width of the *e*-beam pulse.

The *e*-beam response time is the sum of two processes; the slowing of beam electrons and the slowing of beam-generated secondary electrons. The secondary electron response time (SERT) is that value one would observe from a small volume through which an energetic *e* beam has passed and generated a flux of secondary electrons. The SERT is smaller than that of the beam electrons in proportion to the ratio of energy loss cross sections at many keV to that at 10's–100's of eV. This ratio may be many orders of magnitude. To demonstrate this effect the ionizations resulting from only secondary electrons generated by the traversal of a 500-keV beam through a small volume at $t = 0$ is shown in Fig. 10. The gas mixture is $Ar/Kr/F_2 = 90/10/0.25$. The near cessation of ionizations at $t \geqslant 10$ ps atm implies that the SERT is also close to this value. Since secondary electrons may be emitted with energies $\epsilon \leqslant (\epsilon_p - \epsilon_{ion}/2)$ there will be ionizations by secondary electrons at times approaching the beam response time (10's of ns). Their contribution, though, becomes negligibly small at times greater than 10 ps atm. Longer *e*-beam response times are therefore a result of the slowing of beam electrons, and not their secondaries.

e-beam response times which exceed many ns logically require that the beam electrons do not traverse or diffuse out of the observation volume in that time to observe the entire response. If that is not the case, then the apparent *e*-beam response time will likely be smaller than that described here. Its value will be the smaller of the slowing down time and the beam traversal or diffusion time.

VI. CONCLUDING REMARKS

Energy partitioning and *e*-beam response times in electron beam excited plasmas have been discussed using results from a Monte Carlo particle simulation. We find that the practice of obtaining W values in mixtures by using W^0/f becomes increasingly invalid as the differences in the ionization potentials of the gas constituents becomes larger. The actual mole fraction weighted W value for low ionization potential species in mixtures may actually be less than their ionization potential. The *e*-beam response time for beam energies in excess of 100's of keV for pressures of a few atm can exceed 10's of ns. The contributions of inner shell ionization and multiple ionization may decrease the response time, but at most by only $\approx 10\%$. The local secondary electron response time, though, is typically $\ll 1$ ns. The beam response time is therefore largely a result of beam electrons cascading to lower energies. This time may be commensurate with the *e*-beam rise time of long pulse lasers and with the total pulse

length in short pulse lasers. Under these conditions, *e*-beam power deposition cannot be assumed to be instantaneous. In geometrically confined systems, the observed beam response time may, in fact, be the beam traversal (or diffusion) time across the deposition chamber.

ACKNOWLEDGMENTS

This work was supported by Los Alamos National Laboratory under the direction of D. Hanson, and the National Science Foundation (Contract No. ECS 88-15781) under the direction of L. Goldberg.

[1]F. Kannari and W. D. Kimura, J. Appl. Phys. **63**, 4377 (1988).
[2]A. Mandl and E. Salesky, J. Appl. Phys. **60**, 1565 (1986).
[3]A. Hunter, R. Hunter, and T. Johnson, IEEE J. Quantum Electron. **QE-22**, 386 (1986).
[4]A. E. Mandl and H. Hyman, IEEE J. Quantum Electron. **QE-22**, 349 (1986).
[5]A. Suda, M. Obara, and T. Fujioka, Jpn. J. Appl. Phys. **24**, 1183 (1985).
[6]R. Razdan, C. E. Capjak, and H. J. J. Seguin, J. Appl. Phys. **57**, 4954 (1985).
[7]J. P. Boeuf and E. Marode, J. Phys. D **15**, 2169 (1982).
[8]E. E. Kunhardt and C. Wu, J. Comput. Phys. **65**, 279 (1986).
[9]C. B. Opal, W. K. Peterson, and E. C. Beaty, J. Chem. Phys. **55**, 4100 (1971).
[10]J. Bretagne, J. Godart, and V. Peuch, J. Phys. D **15**, 2205 (1982).
[11]M. Hayashi, Nagoya Institute of Technology Report No. IPPJ-AM-19, 1981 (unpublished).
[12]M. Hayashi and T. Nimura, J. Appl. Phys. **54**, 4879 (1983).
[13]P. J. O. Teubner, J. L. Riley, M. C. Tonkin, J. E. Furst, and S. J. Buckman, J. Phys. B **18**, 3641 (1985).
[14]F. J. deHeer, R. H. J. Jansen, and W. vander Kaay, J. Phys. B **12**, 979 (1979).
[15]K. Tachibana, Phys. Rev. A **34**, 1007 (1986).
[16]R. Hyde and M. Roberts, Lawrence Livermore National Laboratory Report No. UCID-1778, 1978 (unpublished).
[17]N. J. Mason and W. R. Newell, J. Phys. B **20**, 1357 (1987).
[18]M. Hayashi, J. Phys. D **26**, 581 (1983).
[19]D. Rapp and P. Englander-Golden, J. Chem. Phys. **43**, 1464 (1965).
[20]D. C. Lorents, Physica **82B**, 19 (1976).
[21]L. G. Christophorou, *Atomic and Radiation Physics* (Wiley, New York, 1971), Chap. 2.
[22]K. S. Jancaitis, Lawrence Livermore National Laboratory Report No. UCRL-53465, 1983 (unpublished).
[23]J. Blauer, T. T. Yang, C. E. Turner, and D. A. Copeland, Appl. Opt. **23**, 4352 (1984).
[24]E. Eggarter, J. Chem. Phys. **84**, 6123 (1986).
[25]M. Inokuti and E. Eggarter, J. Chem. Phys. **86**, 3870 (1987).
[26]R. D. Taylor, S. P. Slinker, and A. W. Ali, J. Appl. Phys. **64**, 982 (1988).
[27]V. A. Adamovick, A. V. Dem'yanov, N. A. Dyatko, I. V. Kochetov, A. P. Napartovich, and A. P. Strel'tsov, Sov. Phys. Tech. Phys. **32**, 568 (1978).
[28]J. P. Novak and M. F. Fréchette, J. Appl. Phys. **57**, 4368 (1985).
[29]L. R. Peterson and J. E. Allen, J. Chem. Phys. **56**, 6068 (1972).
[30]T. D. Märk, in *Electron Impact Ionization*, edited by T. D. Märk and G. H. Dunn (Springer, Wien, 1985), pp. 137–197.
[31]M. J. Berger and S. M. Seltzer, "Tables of Energy Losses and Ranges of Electrons and Positrons," NASA SP-3012, National Aeronautics and Space Administration, 1964 (unpublished).